AAC Journals.ASM.org

Cationic Antimicrobial Peptides and Biogenic Silver Nanoparticles Kill Mycobacteria without Eliciting DNA Damage and Cytotoxicity in Mouse Macrophages

Soumitra Mohanty,[a] Prajna Jena,[a] Ranjit Mehta,[a] Rashmirekha Pati,[a] Birendranath Banerjee,[a] Satish Patil,[b] Avinash Sonawane[a]

School of Biotechnology, KIIT University, Bhubaneswar, Orissa, India[a]; School of Life Sciences, North Maharashtra University, Jalgaon, India[b]

With the emergence of multidrug-resistant mycobacterial strains, better therapeutic strategies are required for the successful treatment of the infection. Although antimicrobial peptides (AMPs) and silver nanoparticles (AgNPs) are becoming one of the popular antibacterial agents, their antimycobacterial potential is not fully evaluated. In this study, we synthesized biogenic-silver nanoparticles using bacterial, fungal, and plant biomasses and analyzed their antibacterial activities in combination with AMPs against mycobacteria. *Mycobacterium smegmatis* was found to be more susceptible to AgNPs compared to *M. marinum*. We found that NK-2 showed enhanced killing effect with NP-1 and NP-2 biogenic nanoparticles at a 0.5-ppm concentration, whereas LLKKK-18 showed antibacterial activity only with NP-2 at 0.5-ppm dose against *M. smegmatis*. In case of *M. marinum* NK-2 did not show any additive activity with NP-1 and NP-2 and LLKKK-18 alone completely inhibited the bacterial growth. Both NP-1 and NP-2 also showed increased killing of *M. smegmatis* in combination with the antituberculosis drug rifampin. The sizes and shapes of the AgNPs were determined by transmission electron microscopy and dynamic light scattering. AgNPs showed no cytotoxic or DNA damage effects on macrophages at the mycobactericidal dose, whereas treatment with higher doses of AgNPs caused toxicity and micronuclei formation in cytokinesis blocked cells. Macrophages actively endocytosed fluorescein isothiocyanate-labeled AgNPs resulting in nitric oxide independent intracellular killing of *M. smegmatis*. Apoptosis and cell cycle studies showed that treatment with higher dose of AgNPs arrested macrophages at the G_1-phase. In summary, our data suggest the combined effect of biogenic-AgNPs and antimicrobial peptides as a promising antimycobacterial template.

Bacterial infections remain a major cause of death, disability, and socioeconomic burden for millions of people worldwide. The genus *Mycobacterium* includes an expanding list of both infectious and saprophytic bacteria that can infect humans and animals. The species causing human diseases include *Mycobacterium tuberculosis*, *M. avium*, *M. bovis*, *M. smegmatis*, and *M. marinum*, whereas *M. bovis* and *M. marinum* also cause disease in cattle and fish, respectively (1). Although tuberculosis is the most common infectious disease caused by *M. tuberculosis*, mycobacteria also cause other diseases such as abscesses, septic arthritis, and osteomyelitis (2, 3). On an annual basis, active cases of tuberculosis account for ~1.5 million deaths and 10 million new cases. Major factors that have contributed to the development of resistance are the emergence of multidrug-resistant strains (4) and the presence of multilayered lipid-rich hydrophobic mycobacterial cell wall structure, which limits the binding or the entry of drug into the cell (5). Moreover, the cell wall of pathogenic mycobacteria contains several efflux systems by which the pathogen can pump out the antibiotics effectively (6, 7). It is thus imperative to design and develop better therapeutic strategies to treat the mycobacterial infections successfully. One of the approaches for successful treatment of mycobacterial infections could be the use of a combination of drugs with different mode of actions. In view of this, antimicrobial peptides (AMPs) and metallic nanoparticles (NPs) have attracted increasing attention due to their potent antibacterial activity.

AMPs, also known as natural antibiotics, constitute an important component of innate immunity against viruses, fungi, and bacteria throughout the animal and plant kingdoms (8, 9). AMPs selectively bind to the bacterial membranes containing substantial amount of acidic phospholipids and other negatively charged molecules (10). As mentioned above, lipids constitute ca. 60% of the mycobacterial cell wall. We have previously shown that several cationic AMPs, such as NK-2 (11), LL-37, and its variant LLKKK-18 (12), exhibit antimycobacterial activity when used as a single drug agent. However, their antibacterial efficacy decreased from nonpathogenic to pathogenic mycobacteria. NK-2 is a peptide representing the cationic core region of the lymphocytic effector protein NK-lysin, which is found in NK cells and cytotoxic T cells (13). NK-2 has been found active against Gram-positive and Gram-negative bacteria, parasitic protozoa such as *Trypanosoma cruzi* (14) and *Plasmodium falciparum* (13) and the fungal pathogen *Candida albicans* (15). LL-37, an amphipathic α-helical peptide, is expressed in neutrophils, macrophages, monocytes, myeloid bone marrow cells, and epithelial cells. We have prepared several variants of LL-37. Among them, a variant (LLKKK-18) in which polar uncharged residues glutamine (Q22), asparagine (N30), and negatively charged aspartic acid (D26) were substi-

Received 11 December 2012 Returned for modification 10 February 2013
Accepted 15 May 2013
Published ahead of print 20 May 2013
Address correspondence to Avinash Sonawane, asonawane@kiitbiotech.ac.in.
S.M. and P.J. contributed equally to this article.
Supplemental material for this article may be found at http://dx.doi.org/10.1128/AAC.02475-12.

doi:10.1128/AAC.02475-12

tuted by positively charged lysine (K) showed more antimycobacterial activity compared to parental LL-37 peptide (12).

Along with AMPs, several metallic nanoparticles, such as silver (16, 17, 18), gold (19, 20), zinc oxide (21, 22), have also emerged as potential alternative for the treatment of drug-resistant bacterial infections. Among them, silver nanoparticles (AgNPs) have attracted great attention in recent years owing to their potent broad-spectrum antimicrobial activity, lower propensity to induce microbial resistance than antibiotics, unique mode of action, and ease of generation (23, 24). AgNP binding disrupt microbial cell wall permeability and affect cellular respiration by forming complexes with the catalytic sulfur groups in cysteine residues (25) and through the production of toxic superoxide radicals (26). The cytotoxic and genotoxic studies showed that the cytotoxicity, DNA damage, chromosome aberrations, and cell death activities of AgNPs enhanced if they are directly applied above a certain concentration level (27). Recently, we have shown that high doses of starch and chitosan-stabilized AgNPs cause significant cytotoxic and genotoxic effect in macrophages (17, 18). Nanoparticles also interact with immune cells and modulate their function to increase the immunotoxicity (28). Macrophages, a primary resident cell for mycobacteria, are notable for their capacity to phagocytose nanoparticles possibly through endocytic pathways, which may lead to intracellular killing of bacteria (29).

To date, numerous chemical methods concerning the fabrication of AgNPs have been developed (30–33). Most of these chemical agents lead to environmental toxicity or biological hazardous risks; therefore, the trend has shifted to biological synthesis of AgNPs using polymer matrices (34), bacterial biomasses (35), fungal biomasses (36), or plant extracts (37) as stabilizing and reducing agents. The biological synthesis of nanoparticles has several advantages over synthetic methods such as they have no toxicity risks and can synthesize stable silver particles that can be easily designed into almost any shape and size required for a particular application.

Although several independent studies have shown applications of AMPs and AgNPs as single antibacterial agent against different human pathogens, no additive analysis of biogenic AgNPs and AMPs against pathogenic and nonpathogenic mycobacteria have been reported. In the present work, we have synthesized biogenic-AgNPs using *Alstonia macrophylla* (NP-1) and *Trichoderma* sp. (NP-2) biomasses and studied their cytotoxic, genotoxic, and antibacterial activities against *M. smegmatis* and *M. marinum* as a single agent or in combination with two potent AMPs, NK-2 and LLKK-18, and the antitubercular drug rifampin. AgNPs were characterized by transmission electron microscopy (TEM) and dynamic light scattering (DLS). We found that the combination of AgNPs and AMPs kill the mycobacteria more efficiently without causing cytotoxicity and genotoxicity effect on mammalian cells as determined by single cell gel electrophoresis (comet), MTT [3-(4,5-dimethylthiazol-2-yl)-2,5-diphenyltetrazolium bromide], nucleus staining, and micronucleus formation assays. Annexin V and cell cycle studies showed that treatment with higher doses of NP-1 and NP-2 arrested cells at the G_1 phase. Moreover, macrophages actively endocytosed fluorescein isothiocyanate (FITC)-labeled AgNPs resulting in nitric oxide (NO) independent intracellular killing of *M. smegmatis*. Altogether, these data support the combinatorial antimycobacterial therapeutic application of AgNPs and AMPs.

MATERIALS AND METHODS

Bacterial and cell line culture conditions. *M. smegmatis* mc2155 (ATCC 700084) and *M. marinum* (ATCC 927) strains were grown in Middlebrook 7H9 broth medium (Difco) supplemented with 10% OADC (oleic acid-albumin-dextrose-catalase) and 0.05% Tween 80 (Merck) at 37 and 30°C, respectively, on a shaker at 120 rpm. The mouse macrophage cell line RAW264.7 was cultured in Dulbecco modified Eagle medium (DMEM; Himedia, Mumbai, India) supplemented with 10% fetal calf serum, 1% penicillin-streptomycin solution, 1% L-glutamine, and HEPES. Low-melting-point agarose, DAPI (4′,6′-diamidino-2-phenylindole), and FITC were purchased from Sigma-Aldrich (St. Louis, MO). MTT was purchased from MP Biomedicals (USA). Silver nitrate solution was purchased from Fisher Scientific (Mumbai, India). Propidium iodide was purchased from Invitrogen.

Antimicrobial peptides. The synthesis of NK-2 and LLKKK-18 having primary structures KILRGVCKKIMRTFLRRISKDILTGKK-NH_2 (11) and H-KEFKRIVKRIKKFLRKL-OH (12), respectively, have been described previously. Stock solution of NK-2 was prepared by dissolving it in 10 mM HCl and further diluted in required buffer or medium during the experiment. LLKKK-18 was dissolved in 0.1% acetic acid.

Synthesis of silver nanoparticles using plant extracts. One-gram portions tender leaves of *Alstonia macrophylla* were cut into small pieces in 10 ml of distilled water. The solution was mixed with 100 ppm of silver nitrate ($AgNO_3$) solution in 0.1% starch under continuous stirring at 50°C. Development of brown color solution indicated the formation of AgNPs. Synthesis of nanoparticles was confirmed by measuring the absorption spectra of the solution at 420 nm and by TEM and DLS analysis.

Synthesis of nanoparticles using *Trichoderma* biomass. For the synthesis of AgNPs using fungi, loopful spores of *Trichoderma* sp. were inoculated in potato dextrose broth (PDB) and incubated for 48 h at 28°C. A 5% cell suspension was inoculated in 500 ml of PDB and incubated for another 24 h. Cell mass was separated by filtration, and a 1-g wet pellet was added in a 100-ppm $AgNO_3$ solution.

Nanoparticle characterization. For TEM, a drop of aqueous solution of AgNPs was placed on the carbon-coated copper grids. The samples were dried and kept overnight under a desiccator before loading them onto a specimen holder. The TEM measurements were performed on a JEM-2100 HRTEM apparatus (JEOL, Japan) operating at 200 kV. The size distribution and zeta potential of the AgNPs were determined by DLS (Zetasizer Nano ZS Malvern Instruments, Malvern, United Kingdom) at room temperature.

***In vitro* killing assay.** *M. smegmatis* and *M. marinum* (4×10^3 to 9×10^3/ml) were grown in the presence of NP-1 and NP-2 with or without NK-2 and LLKKK-18 in Tris-glucose buffer (10 mM Tris, 5 mM glucose [pH 7.4]) supplemented with 0.05% Tween 80 in 96-well plate for 6 h. Before checking the additive activities of NPs and peptides, the MICs of NK-2 and LLKKK-18 against *M. smegmatis* and *M. marinum* were determined by incubating the bacteria with 3.5, 17.5, 35, and 87.5 μg and 1, 5, 10, and 25 μg of peptides/ml, respectively, for 24 h. NPs at concentrations of 0.1 and 0.5 ppm alone or in combination with NK-2 (7 μg/ml) and LLKKK-18 (1 μg/ml) were selected for antibacterial assay. The antimycobacterial activity of NPs and rifampin was checked by incubating 0.1 ppm of NP-1 and NP-2 with or without 0.7 μg of rifampin/ml against *M. smegmatis* and *M. marinum* for 24 h. CFU were assayed by plating 5 μl of suitably diluted samples in triplicate in 7H10 plates supplemented with OADC at the indicated time points and were counted after 3 days. All samples were plated in triplicate, and values were averaged from three independent experiments. Mycobacteria grown in Tris-glucose buffer only served as control.

Cytotoxicity assay. RAW264.7 cells (10^4 cells/well) in DMEM were grown in 96-well plate at 37°C, 5% CO_2 for 24 h, followed by treatment with different concentrations of AgNPs and peptides alone or in combination for another 24 h. To determine the cell viability, MTT (0.1 mg/ml) was added to the wells, followed by incubation for 4 h in dark. In metabolically active cells, MTT was reduced to an insoluble dark purple form-

azan. The formazan crystals were dissolved in dissolving buffer (11 g of sodium dodecyl sulfate in 50 ml of 0.02 M HCl and 50 ml of isopropanol). The absorbance was read at 570 nm in enzyme-linked immunosorbent assay (ELISA) reader (Biotek, Germany), compared to untreated cells, and the percentage of viable cells was calculated.

Comet assay. The effect of AgNPs on DNA damage was determined by alkaline single cell electrophoresis (Comet) assay. Macrophages were treated with a bactericidal agent (5 ppm) and 10 ppm of AgNPs for 12 h. Untreated cells were used as a control. Cells were treated with trypsin, and a cell suspension was prepared in 1× phosphate-buffered saline (PBS). Then, 10 μl of cell suspension was mixed with 60 μl of 0.5% low-melting-point agarose. A thin smear of cell suspension was prepared in glass cavity slides (Blue Label Scientifics, Mumbai, India). The agarose was allowed to solidify in the dark at 4°C for 45 min, and then the slides were submerged in lysis solution (10 mM Tris, 100 mM EDTA, 2.5 M NaCl, 1% Triton X-100, 10% dimethyl sulfoxide) for 30 min in dark at 4°C. After lysis, the slides were washed with distilled H_2O (dH_2O), transferred to an electrophoresis unit containing freshly prepared electrophoresis buffer (500 mM EDTA, 200 mM NaOH [pH >13]), and left for unwinding of DNA for 45 min, and the cells were electrophoresed for 15 min at 15 V. The cells were washed twice with dH_2O, fixed with 70% chilled ethanol, and stained with 0.5 μg of propidium iodide/ml for 15 min in dark. The slides were dried and observed using a fluorescence microscope (Nikon, Japan).

Micronucleus assay. RAW264.7 cells (2×10^5 cells/well) were grown in six-well plates and treated with 5 and 10 ppm of AgNPs for 6 h. Cells grown in media were used as a control. The cells were then processed for micronucleus assay as previously described (38). Briefly, the cells were arrested at the cytokinesis stage by the addition of cytochalasin B (0.5 mg/ml) in 1× PBS at a concentration of 10 μg/ml, and the cells were allowed to grow for 12 h. The cells were then treated with trypsin and centrifuged at 1,000 rpm for 8 min at room temperature. Cells were fixed by the addition of chilled methanol and acetic acid (3:1), vortexed simultaneously, and incubated at 4°C for 1 h. The process described above was repeated twice until the cell suspension appeared clear. Finally, a few drops of cell suspension were added on a slide, air dried, and stained with propidium iodide stain. The images were captured by Olympus BX61 fluorescence microscope using appropriate filters and analyzed by Cytovision7.2 software.

Apoptosis assay. The percentage of apoptotic cells was determined by using an Annexin V-FITC apoptosis detection kit (Sigma). Briefly, 2×10^5 RAW264.7 cells were grown overnight in six-well culture plate (Tarson, India) and treated with 5 and 10 ppm of AgNPs, and the cells were incubated for another 12 h. The cells were treated with trypsin and washed three times with Dulbecco's phosphate-buffered saline (0.1 M [pH 7.4]). A 500-μl portion of 1× binding buffer was added, followed by 5 μl of annexin V-FITC and 10 μl of propidium iodide, and then incubated for 10 min at room temperature in the dark. Untreated cells were taken as a negative control. Flow cytometry was performed by analyzing 10,000 gated cells using a FACSCalibur flow cytometer and CellQuest software (Becton Dickinson [BD], USA).

Free nitric oxide estimation. RAW264.7 cells (2×10^5) were grown overnight in a six-well plate, followed by treatment with 5- and 10-ppm concentrations of AgNPs for another 24 h. The accumulation of nitrite was measured by mixing 100 μl of cell supernatants with an equal volume of Griess reagent (1% sulfanilamide–0.1% naphthylethylenediamine dihydrochloride in 5% concentrated H_3PO_4), followed by incubation for 10 min at room temperature, and the absorbance was measured at 550 nm in a microtiter plate reader (Epoch; Bio-Tek, USA). The nitrite production (in micromoles per liter) was determined by least-square linear regression analysis using sodium nitrite as a standard (5 to 100 μM). Each experiment was performed in triplicate.

Endocytosis and intracellular accumulation of AgNPs in macrophages. AgNPs were labeled by addition of 0.1 μg of FITC/ml, and the mixture was stirred continuously for 8 h at 4°C in dark. FITC-labeled AgNPs were added to RAW264.7 cells (10^5cells/ml) and incubated for 1 h. The cells were fixed with 3.7% paraformaldehyde for 30 min at 37°C, washed with 1× PBS, and mounted on glass slides. The images were visualized by fluorescence microscope. To study the accumulation of nanoparticles, NP-1 and NP-2 were labeled with FITC as described above. The macrophages (5×10^5 cells/ml) were incubated with 1 and 2 ppm of nanoparticles, and the intracellular accumulation of NPs was determined after 12, 24, and 48 h of incubation by flow cytometry using fluorescence-activated cell sorting (FACS; Canto II; BD).

Effect on intracellular killing of mycobacteria. To examine whether treatment with AgNPs and AMPs increase killing efficiency of macrophages, 5×10^5 RAW264.7 cells were infected with *M. smegmatis* and *M. marinum* for 2 h at a multiplicity of infection of 10, followed by killing of extracellular bacteria by addition of 20 μg of gentamicin/ml. Macrophages were treated with NP-1 and NP-2 (0.5 ppm) alone or in combination with NK-2 and LLKKK-18. Macrophages infected with bacteria alone were used as a control. After the incubation period, the cells were washed and lysed with 0.5% Triton X-100. The intracellular survival was determined by plating serially diluted cultures on 7H10 plates, and the colonies were enumerated after 3 days for both *M. smegmatis* and *M. marinum*.

Statistical analysis. Statistically significant differences between groups were determined using the Mann-Whitney U-test (two-tailed, equal variances; **, $P \leq 0.01$; *, $P \leq 0.05$).

RESULTS

Characterization of nanoparticles. Different bacterial, fungal, and plant extracts were used to stabilize and reduce $AgNO_3$ to AgNPs. A total of eight different extracts were used: five from plants, one from bacteria, and two from fungi. The appearance of brown color and maximum UV-absorption spectra at 420 nm indicated the formation of AgNPs. Further microscopic analysis indicated that the optimum synthesis of AgNPs occurred only in the presence of a plant *Alstonia macrophylla* (NP-1) and fungal *Trichoderma* sp. (NP-2) biomasses. Therefore, these two particles were selected for further studies. The shapes of these two particles were determined by TEM. A typical TEM micrograph showed spherical, monodispersed NP-1 and NP-2 particles of 50 and 100 nm, respectively (Fig. 1A). DLS showed predominantly two sizes of NP-1 and NP-2 viz. 177 and 97.65 nm (Fig. 1B), while surface zeta potential was measured as −2.70 and 13 mV, respectively (Fig. 1C).

Antimycobacterial activity of AgNPs in combinations with AMPs and rifampin. Previously, we have shown that the AgNPs synthesized using biopolymers exhibit antibacterial activity against Gram-positive and Gram-negative bacteria (17, 18). It is worth noting that the mycobacteria are resistant to numerous drugs due to lipid-rich cell wall. First, *M. smegmatis* viability was determined in the presence of different doses of NP-1 and NP-2 in 96-well round-bottom plates by a CFU assay. Incubation with higher doses (>0.5 ppm) showed complete killing of bacteria (data not shown). Previously, we have shown that NK-2 and LLKKK-18 exhibit significant antimycobacterial activity (11, 12). First, we determined the *M. smegmatis* viability in the presence of different doses of NK-2 and LLKKK-18. A CFU assay showed that 3.5 μg of NK-2/ml had no significant killing effect, whereas 17.5 μg of NK-2/ml killed >90% *M. smegmatis* population after 24 h of incubation (see Fig. S1A in the supplemental material). In the case of LLKKK-18, no significant killing of *M. smegmatis* was observed in 1- and 5-μg/ml LLKKK-18 treatments, whereas 25 μg of LLKKK-18/ml killed >80% of *M. smegmatis* after 24 h (see Fig. S1A in the supplemental material). *M. marinum* was found to be more susceptible to both NK-2 and LLKKK-18 since ca. 90% of bacterial killing was observed with 3.5 and 1 μg of NK-2 and

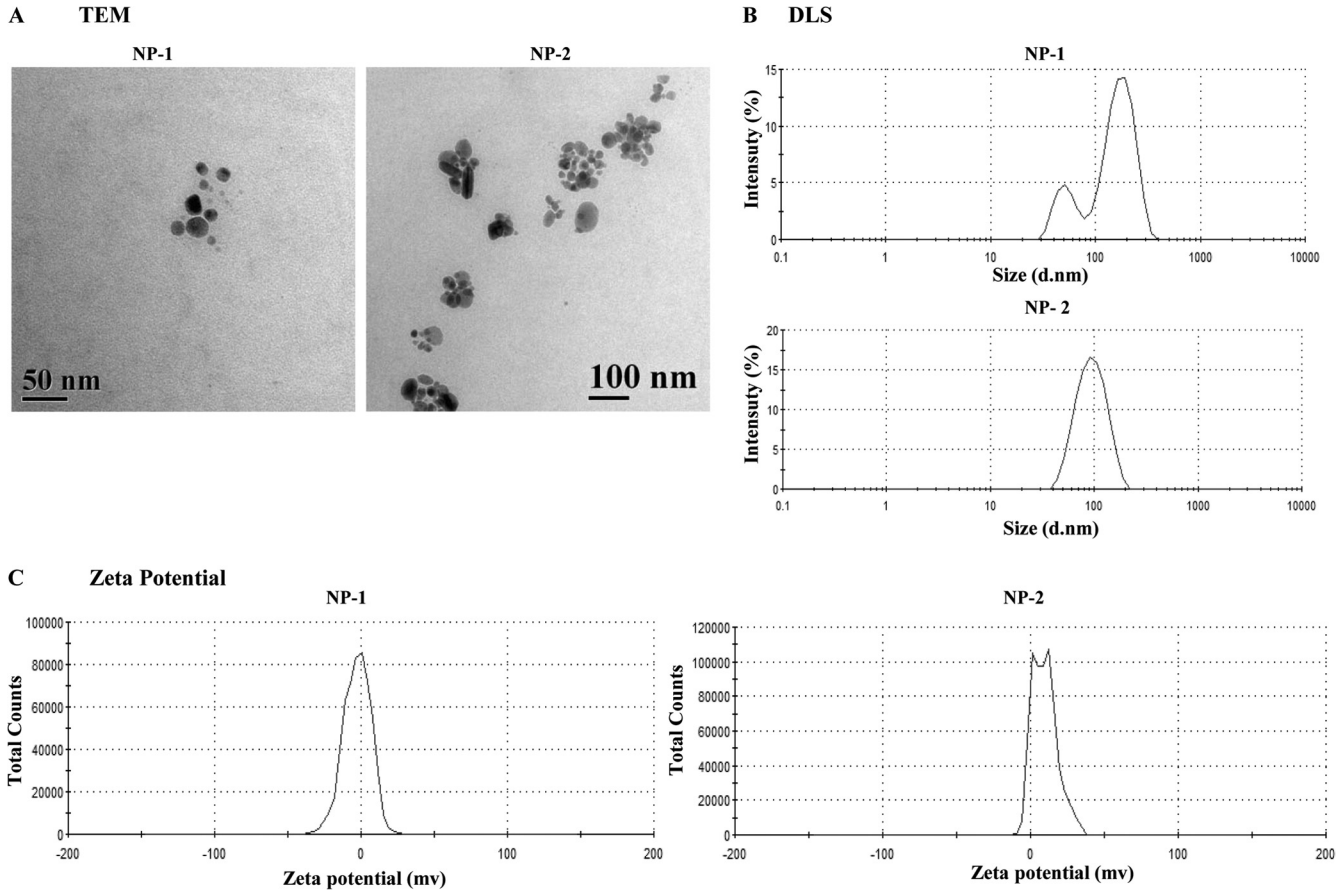

FIG 1 (A) Transmission electron microscopy of NP-1 and NP-2 (scale bars, 50 and 100 nm, respectively). (B) Determination of zeta size distribution of NP-1 and NP-2 by DLS. (C) Zeta potential of NP-1 and NP-2.

LLKKK-18/ml, respectively (see Fig. S1B in the supplemental material). Complete bacterial killing was observed with both NK-2 (17.5, 35, and 87.5 μg/ml) and LLKKK-18 (5, 10, and 25 μg/ml) at higher doses. Therefore, in the present study, we used sublethal doses of NPs (0.1 and 0.5 ppm), NK-2 (7 μg/ml), and LLKKK-18 (1 μg/ml) for antibacterial assays. Exponentially grown bacteria were incubated with 0.1 and 0.5 ppm of NP-1 and NP-2 alone or in combination with NK-2 and LLKKK-18. We also checked the antibacterial activity of NP-1 and NP-2 in combination with rifampin, which is one the most potent first-line antitubercular drugs used for the treatment. Previous investigation has shown that MIC of rifampin ranges between 0.5 and 1 μg/ml (39). Therefore, we selected a sublethal dose (0.7 μg/ml) of rifampin to check the additive effect with NP-1 and NP-2 against *M. smegmatis*. The CFU were analyzed by harvesting bacteria at different time points. The surviving colonies were enumerated after 72 h for *M. smegmatis* and *M. marinum*. The results were compared against a control (no treatment). As shown in Fig. 2A, NP-1 particles showed superior dose-dependent antibacterial activity against *M. smegmatis*. At 0.1- and 0.5-ppm concentrations of NP-1, ca. 60 and 80% of the *M. smegmatis* were killed, respectively, after 6 h of incubation ($P \leq 0.01$), relative to the control. Although under similar conditions NP-2 showed ca. 53 and 75% ($P \leq 0.01$) killing activity. Both the nanoparticles exhibited pronounced antibacterial effect with NK-2, killing more than 90% of *M. smegmatis* at a concentration of 0.5 ppm of NP-1 and NP-2 and 7 μg of NK-2/ml. In the case of LLKKK-18, we found an additive effect with 0.5 ppm of NP-2 only, showing 89% killing of *M. smegmatis*. On the other hand, exposure to NK-2 (7 μg/ml) and LLKKK-18 (1 μg/ml) alone showed moderate bacterial killing after 6 h of incubation (Fig. 2A). Among peptides and nanoparticles, NP-1 and NK-2 was found to kill >50% *M. smegmatis* in an additive manner after 3 h of incubation (see Fig. S1C in the supplemental material). *M. marinum* was found to be slightly more resistant to both NPs such that exposure to 0.5 ppm of NP-1 and NP-2 showed 42 and 65% of bacterial killing, respectively. In the case of peptides alone, *M. marinum* exhibited more sensitivity to LLKKK-18, in which completely bacterial killing was observed after 6 h of incubation (Fig. 2C). After 3 h of incubation, complete killing of *M. marinum* was observed with LLKKK-18 treatment, and no additive effect was found between nanoparticles and peptides (see Fig. S1D in the supplemental material). Since LLKKK-18 alone showed complete killing, we did not perform a combinatorial *in vitro* killing assay with this peptide. Significant killing of *M. smegmatis* was observed after exposure to a combination of rifampin and nanoparticles. The combination of NP-1 (0.1 ppm) and rifampin (0.7 μg/ml) exhibited ~2-fold increased killing of *M. smegmatis* compared to bacteria treated with NP-1 alone after 6 h of

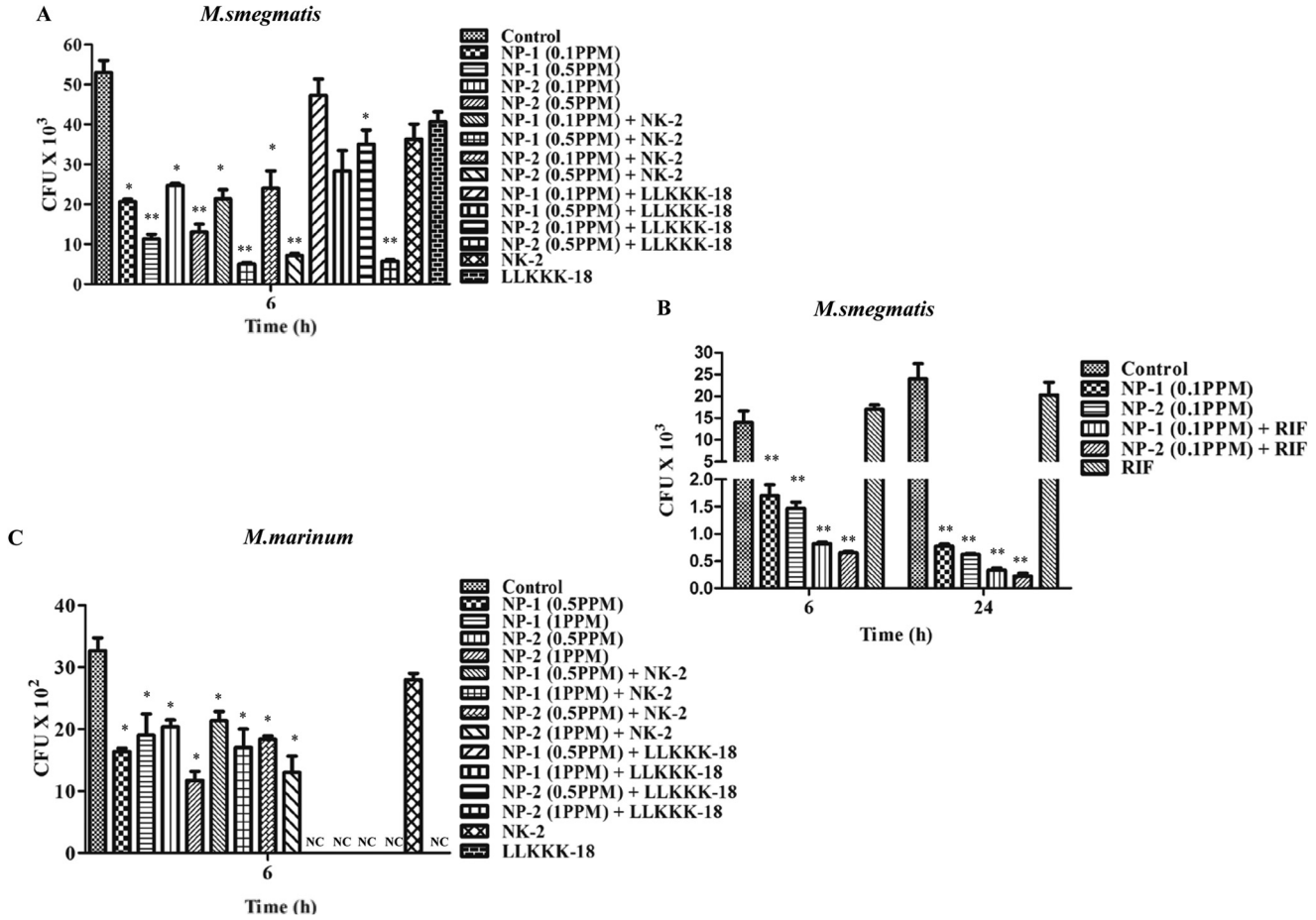

FIG 2 Antibacterial activity of NP-1 and NP-2 against mycobacteria. *M. smegmatis* (A) and *M. marinum* (C) were incubated with different concentrations of nanoparticles (NP-1 and NP-2) and peptides (NK-2 and LLKKK-18) alone and in combinations, and *M. smegmatis* was incubated with 0.1 ppm of nanoparticles with or without rifampin (RIF; 0.7 μg/ml) (B) to check the additive effect. The bacterial survival rate was determined after 6 and 24 h by CFU assay. Medium containing bacteria alone was used as a control. Experiments were performed in triplicates; means ± the standard deviation (SD) are shown. **, $P \leq 0.01$; *, $P \leq 0.05$.

incubation. Similarly, NP-2 in combination with rifampin killed 2.3-fold more of the *M. smegmatis* population compared to NP-2 alone. After 24 h of incubation, the combination of rifampin with NP-1 and NP-2 showed ~2.3- and ~3-fold reductions in bacterial viability, respectively. The combination of NP-1 and NP-2 at 0.5 ppm with 0.7 μg of rifampin/ml led to complete killing of *M. smegmatis* (data not shown). In contrast, no additive effect between nanoparticles and rifampin was noticed against *M. marinum* (data not shown). These results indicate that both nanoparticles exhibit a significant additive effect with both AMPs and rifampin against *M. smegmatis*.

Cytotoxic effect on macrophages. The use of AMPs and AgNPs as therapeutic agents is greatly reduced due to their intrinsic cytotoxic activity toward mammalian cells. The cytotoxic effect of NP-1, NP-2, NK-2, and LLKKK-18 on RAW264.7 macrophages was assessed by an MTT assay, which relies on the principle that metabolically active cells to convert MTT to purple formazan, so the intensity of the dye is directly proportional to the number of viable cells. As shown in Fig. 3A, exposure to effective bactericidal doses of NP-1, NP-2, NK-2, and LLKKK-18 as a single agent or in combination showed no significant reduction in cell viability. To identify the cytotoxic dose, macrophages were treated with higher doses of NPs (up to 10 ppm). We have previously shown that NK-2 and LLKKK-18 did not show cytotoxicity on macrophages at up to 100- and 25-μg/ml concentrations, respectively (11, 12). Treatment with a 5-ppm concentration, which is 10-fold above the effective bactericidal dose, did not show a cytotoxic effect on macrophages (Fig. 3A). The microscopic examination of monolayer macrophages also showed no distinct morphological changes in cells treated with a 5-ppm concentration (Fig. 3B). However, at a 10-ppm concentration, the cells appeared more rounded and fragmented. Moreover, the cell membrane integrity was determined by trypan blue exclusion assay. A total of 500 cells from three independent experiments were analyzed for trypan blue staining. At 5 ppm or lower doses, statistically no significant differences in the trypan blue-positive cells were observed compared to untreated (control) cells (Fig. 3C), whereas at 10 ppm >90% cells were found to be trypan blue positive.

Genotoxic activity. (i) Nuclear integrity. Many studies have shown that AgNPs, when applied above a certain concentration, cause cell death by loss of nuclear integrity, by DNA damage, or by inducing the death pathways. For toxicity studies, we used either 5 ppm (maximal nontoxic dose) or 10 ppm (toxic dose). First, we determined nuclear integrity by DAPI staining. The cells were

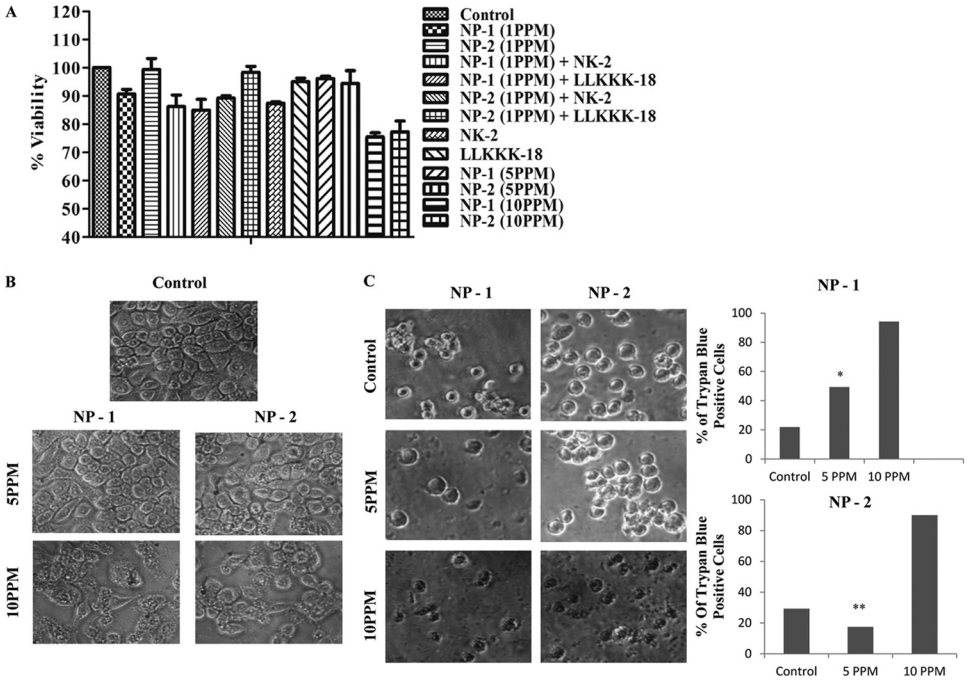

FIG 3 (A) Cytotoxic activity of NP-1, NP-2, NK-2, and LLKKK-18 on RAW264.7 cells. Macrophages were treated with different doses of nanoparticles for 24 h, and cell viability was determined by using an MTT assay. (B) Monolayer morphology of RAW264.7 after treatment with 5- and 10-ppm doses of NP-1 and NP-2. Cells grown in medium were used as a control. (C) Determination of macrophage cell viability by trypan blue exclusion assay. Cells were treated with 5- and 10-ppm doses of NP-1 and NP-2 for 6 h, and the number of trypan blue-positive cells were calculated. Experiments were performed in triplicates; means ± the SD are shown. **, $P \leq 0.01$; *, $P \leq 0.05$.

treated with different doses of NP-1 and NP-2 for 6 h. An intact nucleus was observed in 5-ppm-treated cells. However, at 10 ppm, prominent nucleus shrinkage was observed in NP-1-treated cells compared to NP-2-treated cells (Fig. 4A).

(ii) DNA damage and micronuclei formation. Higher doses of AgNPs exert DNA damage by causing double-strand breaks. Therefore, the effect of AgNPs on macrophage DNA damage was studied using a comet assay. In this assay, the length of the tail increases with the extent of DNA damage. NP-1- and NP-2-treated cells showed a concentration-dependent increase in tail length compared to control cells. No significant DNA damage was observed in control and 5-ppm NP-1- and NP-2-treated cells, whereas a comet-like tail, which implies DNA damage, was observed at a 10-ppm concentration (Fig. 4B).

To corroborate the DNA damage studies, a micronucleus formation assay was performed. A total of 1,000 binucleated cells were analyzed for detecting micronuclei frequency per dose of treated samples. The extent of DNA damage was much higher in cells treated with 10 ppm of NP-1, in which significant numbers of micronuclei were formed, compared to untreated cells and cells treated with 5 ppm (Fig. 4C). Notably, no micronucleus formation was observed in cells treated with 10 ppm of NP-2.

(iii) Cell apoptosis. To examine the nature of cell death, annexin V-FITC/PI dual-staining assay was performed according to the manufacturer's instructions. This dual-staining method differentiates early apoptotic (annexin V-FITC positive, PI negative), necrotic (annexin V-FITC positive, PI positive), and viable cells (annexin V-FITC negative, PI negative) based on the staining pattern. The cells were treated with 5 and 10 ppm of NP-1 and NP-2 for 12 h and analyzed by flow cytometry. The data from the dual-staining experiment showed that only a small percentage (between 13 and 15%) of cells, which is comparable to the control, were undergoing cell death after treatment with 5 ppm, although at 10 ppm an increase in the percent cell death viz. 51 and 40% in NP-1 and NP-2, respectively, was observed (Fig. 4D).

Another important method to assess the DNA damage is to check the cell cycle pattern. Cell cycle arrest leads to apoptotic and necrotic cell death. As shown in Fig. 4E, no significant differences in the cell cycle pattern were observed in 5 ppm of NP-1- and NP-2-treated cells compared to control cells. However, treatment with 10 ppm of NP-1 showed the presence of 37.6% of cells in GO phase in contrast to ca. 0.5% cells in control and NP-2-treated cells. Moreover, exposure of macrophages to 10 ppm of NP-1 particles indicated that the cells may be blocked at the G_1-phase checkpoint, whereas no differences in the cell cycle were observed in NP-2-treated and control cells (Fig. 4E).

Intracellular killing of mycobacteria in nanoparticle- and peptide-treated macrophages. Macrophages can endocytose any particle ranging from 100 nm up to 10 μm. First, we performed immunofluorescence studies using FITC-labeled nanoparticles to evaluate the internalization of exogenously added NP-1 and NP-2 by macrophages. Our microscopic studies showed uptake of both particles by macrophages (Fig. 5A). Uptake of both nanoparticles was further confirmed by FACS analysis. We observed that 1.8% of NP-1 was endocytosed by macrophages, where as an increased rate of NP-2 (15.2%) was observed after 12 h of incubation (Fig. 5D). After 24 and 48 h of treatment, no further increase in the uptake of both NPs was observed (Fig. 5D). In fact, negligible amount of NPs was found inside the macrophages, indicating that NPs may be degraded by intracellular lysosomal enzymes.

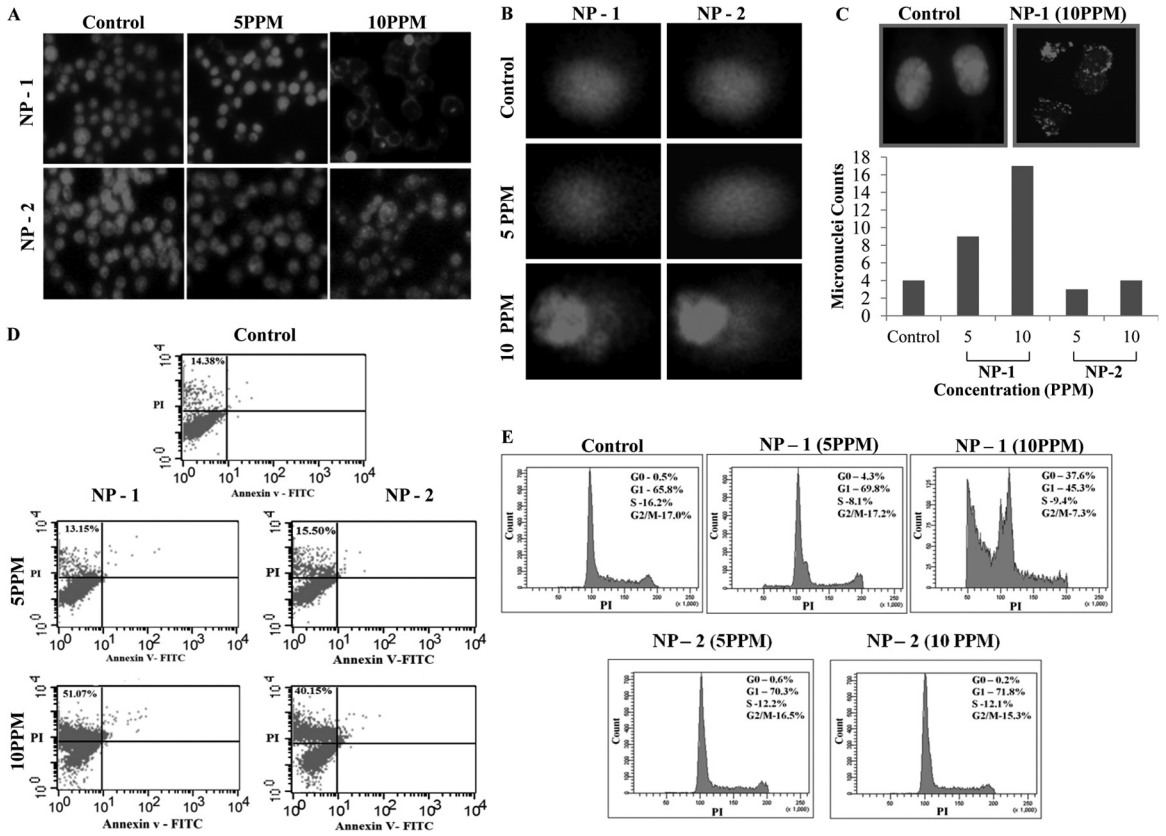

FIG 4 Genotoxic activity of NP-1 and NP-2 on RAW264.7 cells. (A) Nuclear staining of control macrophages (untreated) and macrophages treated with 5 and 10 ppm of NP-1 and NP-2 after 6 h. (B) Comet assay of control macrophages (untreated) and macrophages treated with 5 and 10 ppm of NP-1 and NP-2 and then stained with propidium iodide (0.5 μg/ml). (C) Micronucleus formation assay of control macrophages (untreated) and macrophages treated with 5 and 10 ppm of NP-1 and NP-2. (D) Analysis of apoptosis and necrosis in macrophages treated with NP-1 and NP-2 by the annexin V FITC and PI dual-staining method. (E) Cell cycle studies of NP-1- and NP-2-treated macrophages. The cells were stained with propidium iodide.

To test the intracellular survival of mycobacteria, *M. smegmatis*-infected macrophages were treated with 0.5 ppm of NP-1 and NP-2, 7 μg of NK-2/ml, and 1 μg of LLKKK-18/ml alone or in combination. As shown above, these concentrations of nanoparticles and peptides were found to be nontoxic to the macrophages but killed mycobacteria effectively under *in vitro* condition. NP-1 and NP-2 showed ca. 35% reduction in intracellular survival of *M. smegmatis* (Fig. 5B). Interestingly, treatment with a combination of nanoparticles and peptides displayed differential intracellular killing patterns in macrophages. NP-1 in combination with LLKKK-18 was found to be potentially effective, killing ca. 65% of mycobacteria compared to NP-1 or LLKKK-18 alone. On the other hand, NP-2 in combination with NK-2 killed >52% intracellular *M. smegmatis*. Combination of NP-1 and NK-2 showed similar killing pattern to that of nanoparticles alone. No significant reduction in intracellular survival of *M. smegmatis* was observed in NK-2- and LLKKK-18-treated conditions (Fig. 5B). We did not check the intracellular survival of *M. smegmatis* for a prolonged period of time after infection because previous findings have shown that macrophages efficiently kill *M. smegmatis* after 12 h of infection and that, after 24 h, the majority of the bacteria are cleared by macrophages (12, 40, 41). The intracellular killing pattern of *M. marinum* was found to be different compared to *M. smegmatis*. After 6 h of treatment, no significant reduction in intracellular survival of *M. marinum* was observed, although a moderate increase in bacterial killing was observed in NP-2- and NK-2-treated macrophages (Fig. 5C).

Quantification of free nitric oxide production. Macrophages kill intracellular mycobacteria by the production of superoxide radicals such as NO. Therefore, the level of NO production was checked in nanoparticle-treated macrophages. The supernatants of macrophages treated with different doses of NP-1 and NP-2 for 48 h were used to measure the free nitrite formation, which serves as an indirect indicator of NO production. As shown in Fig. 5E and Fig. S2 in the supplemental material, no significant nitrite accumulation was observed after exposure to NP-1 and NP-2 particles for up to 12 h of treatment, whereas after 24- and 48-h exposures, a dose-dependent decrease in NO production was observed.

DISCUSSION

Emergence of multidrug-resistant bacterial strains has become a major problem worldwide. To counteract such infections, it is necessary to develop new therapeutic approaches that will subjugate the limitations of the present drugs. One such approach would be to impregnate a combinatorial therapy with distinctive mode of action. In case of mycobacteria, the hydrophobic nature of the cell wall reduces the binding and permeability of antituberculosis drugs, thereby impairing their bactericidal action. Therefore, it is of utmost importance to find out molecules that will act directly on the cell wall of mycobacteria. In our previous studies,

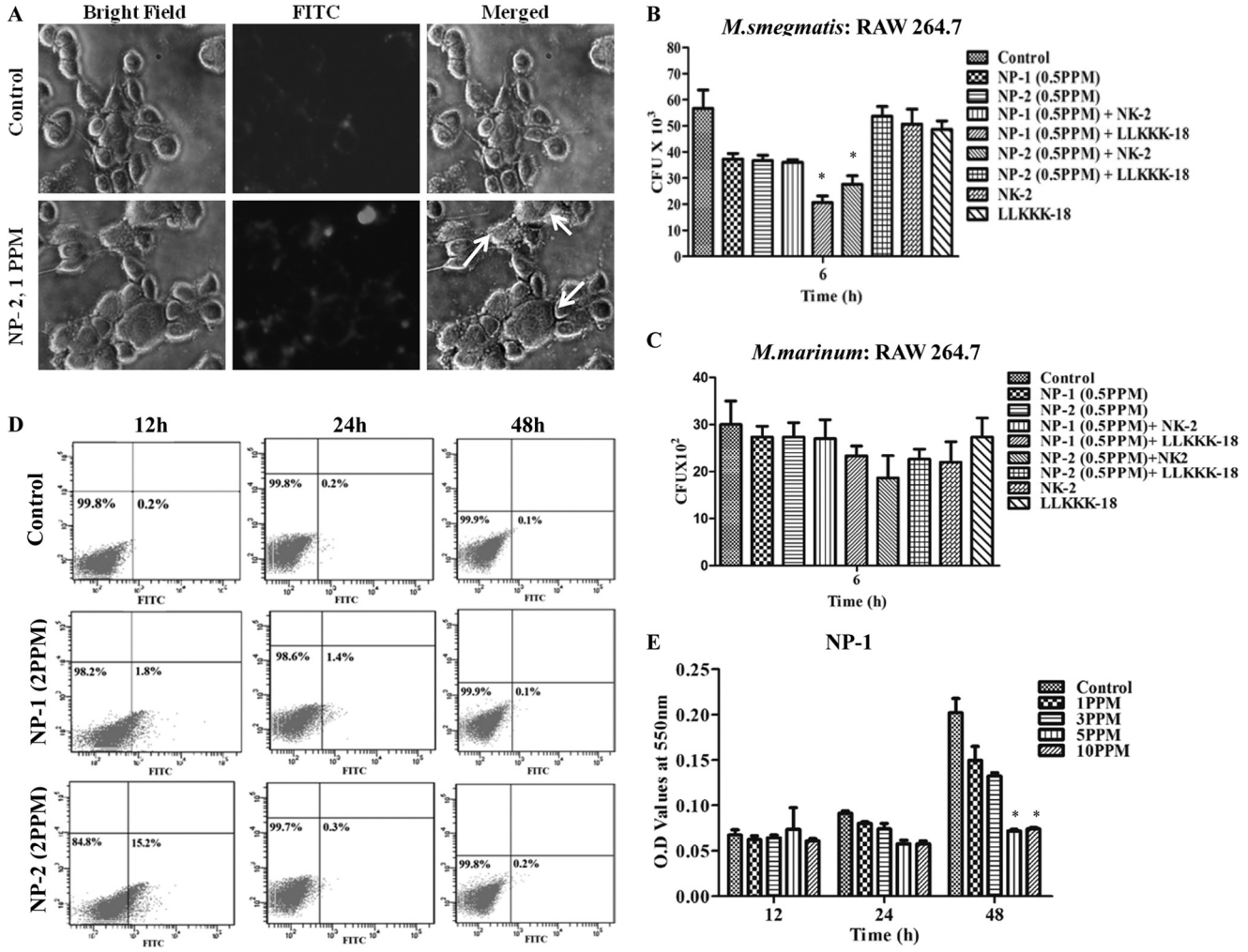

FIG 5 Uptake of nanoparticles and intracellular killing of mycobacteria in macrophages. (A) Arrow mark indicates the intracellular localization of FITC-labeled NP-2. RAW264.7 macrophages were infected with *M. smegmatis* (B) and *M. marinum* (C) for 2 h and then incubated with different concentrations of NP-1 and NP-2. Macrophages infected with bacteria alone were used as a control. Cells were lysed, and bacterial intracellular survival was determined by CFU assay after 6 h. (D) RAW264.7 macrophages were incubated with FITC-labeled nanoparticles for 48 h. Percentage of FITC-positive cells were enumerated through flow cytometry with 10,000 gated cells. (E) Quantification of free nitric oxide production in NP-1-treated macrophages using Griess reagent. Lipopolysaccharide (LPS)-treated and untreated cells were used as positive and negative controls, respectively. Experiments were performed in triplicates. Means ± the SD are shown; *, $P \leq 0.05$.

we have shown that AMPs and metallic nanoparticles kill several human pathogens by permeabilizing the cell membrane (11, 12, 17, 18). Although several reports are available on the antibacterial activity of AgNPs and AMPs against Gram-positive and Gram-negative bacteria, there are no reports that concomitantly describe antimycobacterial, cytotoxic, and genotoxic effects of AMPs and biogenic-AgNPs. We synthesized cost-effective, stable, and potent AgNPs using various bacterial, fungal, and plant extracts as stabilizing and reducing agents. These AgNPs are homogeneous and stable for longer duration as determined by DLS and TEM studies, indicating that plant and bacterial extracts can be used as capping agent to prevent aggregation and increase the solubility of nanoparticles. In this study, we tested additive antibacterial, cytotoxic, and genotoxic activities of NK-2, LLKKK-18, and biogenic AgNPs. It is interesting to observe that nonpathogenic *M. smegmatis* and pathogenic *M. marinum* differ in their susceptibility to antibacterial action of AMPs and AgNPs. Both NP-1 and NP-2 showed additive effects with NK-2 peptide only at a higher concentration (0.5 ppm), whereas a combination of NPs and LLKKK-18 abated the antibacterial activity against *M. smegmatis*. This indicates that NK-2 shows an additive effect only above a certain concentration of NPs. In the case of *M. marinum*, no additive activity was observed with both AgNPs and NK-2, whereas LLKKK-18 alone showed complete bacterial killing. This discrepancy could be due to differences in the properties of AMPs and NPs and the cell wall composition of both bacterial strains (42). AMPs act on cell membrane by forming stable pores after inserting into the membrane or by forming transient pores by destructing phospholipids bilayers. Both the peptides differ in size (Fig. 1), net charge (NK-2, +9; LLKKK-18, +8), and hydrophobicity (NK-2, 40%; LLKK-18, 29% hydrophobic amino acids). Moreover, NP-1 and NP-2 has negative (−2.70 mV) and positive (+13 mV) zeta potential, respectively. These compounded properties may be affecting the interactions between the two molecules and

subsequently the penetration potency into mycobacterial cell wall to achieve the cell death. The fact that LLKKK-18 is more active against a pathogenic *M. marinum* gives a clue that this peptide may also be an excellent antibacterial substance against *M. tuberculosis*. One of the important properties of some AMPs is their ability to act either synergistically or antagonistically on the target cell. We observed a decrease in *M. smegmatis* killing after treatment with a combination of AgNPs and LLKKK-18, indicating an antagonist effect on the target cell. Treatment with a combination of NPs and rifampin also displayed additive effect against *M. smegmatis*. Rifampin kills mycobacteria by binding to the β subunit of the RNA polymerase, thus interfering in RNA synthesis. Mechanistically, it appears that permeabilization of the outer membrane of mycobacteria by membrane-active nanoparticles might enhance penetration of rifampin inside the cells and block the RNA synthesis. Moreover, AMPs also act on the cell membrane of bacteria. NPs are known to kill bacteria by penetrating the bacterial cell membrane, followed by interfering in intracellular ATP production and inhibition of DNA replication. The additive effect of NPs and AMPs could be due to an increase in permeabilization of the bacterial cell membrane by AMPs, which facilitates better penetration of NPs. Moreover, NPs are also known to induce oxidative stress in bacteria. These properties will eventually lead to the killing of bacteria.

One of the important properties of the antibacterial molecule is that it should clear the infection without exerting toxic effect on the host cells. Several AMPs and NPs, such as silver, gold, and zinc oxide, show potent antimicrobial activity accompanied by toxicity on host cells. The cytotoxic effect of AMPs and AgNPs varies with the type of mammalian cells and is largely dependent on AgNP preparation methodologies (43). It was shown that AgNPs that did not contain any surface modifiers or stabilizers showed significant cytotoxic effect on mouse macrophage J774.A1 (44, 45), whereas starch-capped AgNPs had no effect on cancer cells and fibroblasts due to slow release of silver ions from the gel matrix (27). The most noticeable response of cells to toxic molecules is the decrease in metabolic activities, the release of injury signature molecules, and an alteration in cell morphology and shape. We found that NK-2, LLKKK-18, NP-1, and NP-2 at the mycobactericidal dose had no cytotoxic effect on mouse macrophages. These results indicate the suitability of AMPs and biogenic-AgNPs as an antimycobacterial molecule. In comparison, NP-1 was found to be moderately more toxic. The toxicity of nanoparticles differs significantly according to their type, size, release of Ag^+ from nanoparticles, and the capping agent (46–49). Although the shapes of NP-1 and NP-2 were relatively similar (spherical), their size distribution was significantly different. About 80% of NP-1 particles were measured at 177 nm and 20% at 53 nm, whereas NP-2 particles were more homogeneous at 97 nm. Previous reports suggest that AgNPs are more toxic to mammalian cells compared to AMPs. Therefore, we determined the highest noncytotoxic dose of AgNPs. We found that treatment of up to 5 ppm of AgNPs, which is 10-fold more than the effective mycobactericidal dose of NPs, did not show any toxic effect on macrophages. However, treatment with 10 ppm showed a reduction in cellular metabolic activities and disintegration of membrane integrity. This could be due to disturbances in cytoskeletal functions as a result of nanoparticle treatment.

The comet and micronuclei formation assays showed no DNA damage at the mycobactericidal dose (up to 5 ppm), whereas treatment with higher doses (10 ppm) of NP-1 and NP-2 showed significant increases in tail length and micronucleus formation, which manifests DNA damage. It has been observed that exposure to higher doses of AgNPs lead to an increase in DNA damage, apoptosis, and necrosis (27, 50). After DNA damage in the form of strand breaks, micronucleus formation could arise during metaphase/anaphase transition of mitosis, detachment of acentric fragment due to chromosome breakage or from induction of DNA fragmentation, and cell apoptosis. These results were further corroborated by apoptosis assay. No cell apoptosis was observed at the mycobactericidal dose, whereas treatment with higher doses resulted in an increase in the number of apoptotic cells. The increased DNA damage, apoptosis, and micronucleus formation at higher doses could also be due to increased production of reactive oxygen species (ROS). It has been previously reported that increased ROS production due to starch capped AgNPs caused genotoxic effect in fibroblast cells (27). Altogether, these results indicate that NP-1 and NP-2 have no cytotoxic and genotoxic effects on macrophages at the bactericidal dose but when applied above a certain concentration they cause toxic effects.

Owing to their phagocytic function, macrophages can readily ingest foreign material. Macrophages have been shown as an ideal candidate for transporting antiretroviral therapeutic molecules (51). Since mycobacteria are an intracellular pathogen that reside in the phagosomal compartments of macrophages, it is important to deliver the therapeutic molecules to the target sites that would otherwise be inaccessible due to the presence of physical barriers. Recently, it has been shown that AgNPs are actively taken up by the J774A.1 through scavenger receptor-mediated endocytosis (52). Our immunofluorescence studies also showed that FITC-labeled AgNPs are actively endocytosed by macrophages. The shapes and sizes of NPs directly influence their uptake in to the cells (53, 54, 55). Our flow cytometry studies have shown significantly more internalization of FITC-conjugated NP-2 by macrophages compared to NP-1 after 12 h of treatment. However, after 48 h of treatment, negligible amounts of NP-1 and NP-2 were present inside the macrophages. From a therapeutic perspective, this is an important observation because persistent bioaccumulation of AgNPs inside the host cells may cause undesired side effects. Several evidences have suggested that, after endocytosis, NPs are trafficked to the lysosomal compartment through the endocytic pathway, where they are degraded by the action of proteases such as cathepsin L (56). The exogenous addition of NP-1 and NP-2 was found to kill intracellular *M. smegmatis*, whereas intracellular killing was further potentiated after treatment with a combination of NP-1 plus LLKKK-18 and NP-2 plus NK-2. The fact that NP-1 at higher concentrations did not show enhanced killing effect with LLKKK18 under *in vitro* condition, whereas this combination exerted intracellular killing activity under *ex vivo* conditions. Both NPs and AMPs exert immunomodulatory and antigenic activity. The killing of *M. smegmatis* under *ex vivo* conditions could be due to the immunomodulation and/or activation of macrophages or to delivery of endocytosed AgNPs and AMPs to macrophage phagosomes where *M. smegmatis* resides. However, we could not demonstrate enhanced intracellular killing of bacteria due to the antigenic nature of NPs because of limitations in producing NP specific antibodies to neutralize their effect. As mentioned above, the absence of antibacterial activity under *in vitro* conditions could be due to antagonistic effects. Treatment with AMPs and AgNPs also induces the production of

interleukin-1 (IL-1), IL-6, and tumor necrosis factor alpha (47) cytokines, which activate the cells, resulting in an increase in killing efficiency of macrophages. Macrophages kill mycobacteria by inducing NO production. However, no increase in NO production was observed in nanoparticle-treated macrophages, indicating that intracellular mycobacterial killing is NO independent. NPs are also known to induce reactive oxygen species production and the secretion of proinflammatory cytokines. Thus, the observed killing effect could be due to the formation of superoxide radicals and the activation of macrophages by cytokines. In summary, our results demonstrate that the AMPs and NPs tested exhibit at least an additive effect and could be used as potential templates for the treatment of mycobacterial infection. However, in order to prove their therapeutic potential, these AMPs and NPs need to be tested against pathogenic *M. tuberculosis*.

ACKNOWLEDGMENTS

We thank all of the lab members for fruitful discussions and suggestions.

This study was supported by grant BT/PR5790/MED/29/602/2012 from the Department of Biotechnology and SR/NM/NS-1085/2011 from the Department of Science and Technology, Government of India, to A.S. The senior research fellowship from CSIR, Government of India, to S.M. and P.J. is acknowledged.

REFERENCES

1. **Bercovier H, Vincent V.** 2001. Mycobacterial infections in domestic and wild animals due to *Mycobacterium marinum*, *M. fortuitum*, *M. chelonae*, *M. porcinum*, *M. farcinogenes*, *M. smegmatis*, *M. scrofulaceum*, *M. xenopi*, *M. kansasii*, *M. simiae*, and *M. genavense*. Rev. Sci. Technol. **20:**265–290.
2. **Williams B, Neth O, Shingadia D, Dixon G, Jupp RS, Rosendahl K, Eastwood D, Klein N, Brogan P.** 2010. *Mycobacterium kansasii* causing septic arthritis and osteomyelitis in a child. Pediatr. Infect. Dis. **1:**88–89.
3. **Barton A, Bernstein RM, Struthers JK, O'Neill TW.** 1997. *Mycobacterium marinum* infection causing septic arthritis and osteomyelitis. Br. J. Rheumatol. **11:**1207–1209.
4. **Gandhi NR, Nunn P, Dheda K, Schaaf HS, Zignol M, van Soolingen D, Jensen P, Bayona J.** 2010. Multidrug-resistant and extensively drug-resistant tuberculosis: a threat to global control of tuberculosis. Lancet **375:**1830–1843.
5. **Jarlier V, Nikaido H.** 1994. Mycobacterial cell wall: structure and role in natural resistance to antibiotics. FEMS Microbiol. Lett. **123:**11–18.
6. **Da Silva PEA, Von Groll A, Martin A, Palomino JC.** 2011. Efflux as a mechanism for drug resistance in *Mycobacterium tuberculosis*. FEMS Immunol. Med. Microbiol. **63:**1–9.
7. **Garcia SR, Martin C, Thompson CJ, Ainsa JA.** 2009. Role of the *Mycobacterium tuberculosis* P55 efflux pump in intrinsic drug resistance, oxidative stress responses, and growth. Antimicrob. Agents Chemother. **53:** 3675–3682.
8. **Bals R, Fontes W.** 2003. Cathelicidins: a family of multifunctional antimicrobial peptides. Cell. Mol. Life Sci. **4:**711–720.
9. **Casto MS, Fontes W.** 2005. Plant defense and antimicrobial peptides. Protein Pept. Lett. **1:**13–18.
10. **Matsuzaki K.** 1999. Why and how are peptide-lipid interactions utilized for self defense? Magainins and tachyplesin as archetypes. Biochim. Biophys. Acta **1462:**1–10.
11. **Jena P, Mishra B, Leippe M, Hasilik A, Griffiths G, Sonawane A.** 2011. Membrane-active antimicrobial peptides and human placental lysosomal extracts are highly active against mycobacteria. Peptides **32:**881–887.
12. **Sonawane A, Santos JC, Mishra BB, Jena P, Progida C, Sorensen OE, Gallo R, Appelberg R, Griffiths G.** 2011. Cathelicidin is involved in the intracellular killing of mycobacteria in macrophages. Cell. Microbiol. **13:** 1601–1617.
13. **Gelhaus C, Jacobs T, Andra J, Leippe M.** 2008. The antimicrobial peptide NK-2, the core region of mammalian NK-lysin, kills intraerythrocytic *Plasmodium falciparum*. Antimicrob. Agents Chemother. **5:**1713–1720.
14. **Jacobs T, Bruhn H, Gaworski I, Fleischer B, Leippe M.** 2003. NK-lysin and its shortened analog NK-2 exhibit potent activities against *Trypanosoma cruzi*. Antimicrob. Agents Chemother. **47:**607–613.
15. **Andra J, Leippe M.** 1999. Candidacidal activity of shortened synthetic analogs of ameobapores and NK-lysin. Med. Microbiol. Immunol. **188:** 117–124.
16. **Ansari MA, Khan HM, Khan AA, Malik A, Sultan A, Shahid M, Shujatullah F, Azam A.** 2011. Evaluation of antibacterial activity of silver nanoparticles against MSSA and MRSA on isolates from skin infections. Biol. Med. **2:**141–146.
17. **Mohanty S, Mishra S, Jena P, Jacob B, Sarkar B, Sonawane A.** 2012. An investigation on the antibacterial, cytotoxic, and antibiofilm efficacy of starch-stabilized silver nanoparticles. Nanomedicine **6:**916–924.
18. **Jena P, Mohanty S, Mallick R, Jacob B, Sonawane A.** 2012. Toxicity and antibacterial assessment of chitosan-coated silver nanoparticles on human pathogens and macrophage cells. Int. J. Nanomed. **7:**1805–1818.
19. **Pissuwan D, Cortie CH, Valenzuela SM, Cortie MB.** 2009. Functionalized gold nanoparticles for controlling pathogenic bacteria. Trends Biotechnol. **28:**207–213.
20. **Gil-Tomas J.** 2007. Lethal photosensitization of *Staphylococcus aureus* using a toluidine blue *O*-tiopronin-gold nanoparticle conjugate. J. Mater. Chem. **17:**3739–3746.
21. **Liu Y, He L, Mustapha A, Li H, Hu ZQ, Lin M.** 2009. Antibacterial activities of zinc oxide nanoparticles against *Escherichia coli* 0157:H7. J. Appl. Microbiol. **107:**1193–1201.
22. **Jin T, Sun D, Su Y, Zhang H, Sue HJ.** 2009. Antimicrobial efficacy of zinc oxide quantum dots against *Listeria monocytogenes*, *Salmonella enteritidis*, and *Escherichia coli* O157:H7. J. Food Sci. **74:**46–52.
23. **Panacek A, Kvítek L, Prucek R, Kolar M, Vecerova R, Pizúrova N, Sharma VK, Nevecna T, Zboril R.** 2006. Silver colloid nanoparticles: synthesis, characterization, and their antibacterial activity. J. Phys. Chem. B **110:**16248–16253.
24. **Sharma VK, Yngard RA, Lin Y.** 2009. Silver nanoparticles: green synthesis and their antimicrobial activities. Adv. Colloid Interface Sci. **145:** 83–96.
25. **Feng QL, Wu J, Chen GQ, Cui FZ, Kim TN, Kim JO.** 2000. A mechanistic study of the antibacterial effect of silver ions on *Escherichia coli* and *Staphylococcus aureus*. J. Biomed. Mater. Res. **52:**662–668.
26. **Kim JS, Kuk E, Yu KN, Kim JH, Park SJ, Lee HJ, Kim SH, Park YK, Park YH, Hwang CY, Kim YK, Lee YS, Jeong DH, Cho MH.** 2007. Antimicrobial effect of silver nanoparticles. Nanomedicine **3:**95–101.
27. **AshaRani PV, Low Kah Mun G, Hande MP, Valiyaveettil S.** 2009. Cytotoxicity and genotoxicity of silver nanoparticles in human cells. ACS Nano. **3:**279–290.
28. **Arora S, Jain J, Rajwade JM, Paknikar KM.** 2008. Cellular responses induced by silver nanoparticles: in vitro studies. Toxicol. Lett. **179:**93–100.
29. **Iversen TG, Skotland T, Sandvig K.** 2011. Endocytosis and intracellular transport of nanoparticles: present knowledge and need for future studies. Nano Today **6:**176–185.
30. **Kuo PL, Chen WF.** 2011. Formation of silver nanoparticles under structured amino groups in pseudo-dendritic poly(allylamine) derivatives. J. Phys. Chem. B **107:**11267–11272.
31. **Kong H, Jang J.** 2008. Antibacterial properties of novel poly(methyl methacrylate) nanofiber containing silver nanoparticles. Langmuir **24:** 2051–2056.
32. **Chen M, Wang LY, Han JT, Zhang JY, Li ZY, Qian DJ.** 2006. Preparation and study of polyacrylamide-stabilized silver nanoparticles through a one-pot process. J. Phys. Chem. B **110:**11224–11231.
33. **Lu Y, Mei Y, Schrinner M, Ballauff M, Möller MW, Breu J.** 2007. *In situ* formation of Ag nanoparticles in spherical polyacrylic acid brushes by UV irradiation. J. Phys. Chem. **111:**7676–7681.
34. **Fayaz AM, Balaji K, Girilal M, Yadav R, Kalaichelvan PT, Venketesan R.** 2010. Biogenic synthesis of silver nanoparticles and their synergistic effect with antibiotics: a study against Gram-positive and Gram-negative bacteria. Nanomedicine **6:**103–109.
35. **Karmakar S, Kundu S, Kundu K.** 2010. Bioconversion of silver salt to silver nanoparticles using different microorganisms. Artif. Cells Blood Substit. Immobil. Biotechnol. **38:**259–266.
36. **Salunkhe RB, Patil SV, Salunke BK, Patil CD, Sonawane AM.** 2011. Studies on Silver accumulation and nanoparticle synthesis by *Cochliobolus lunatus*. Appl. Biochem. Biotechnol. **165:**221–234.
37. **Dipankar C, Murugan S.** 2012. The green synthesis, characterization and evaluation of the biological activities of silver nanoparticles synthesized from *Iresine herbstii* leaf aqueous extracts. Colloids Surf. B Biointerfaces **98:**112–119.

38. **Fenech M.** 2007. Cytokinesis-block micronucleus cytome assay. Nat. Protoc. **2:**1084–1104.
39. **Bemer-Melchior P, Bryskier A, Drugeon HB.** 2000. Comparison of the *in vitro* activities of rifapentine and rifampicin against *Mycobacterium tuberculosis* complex. J. Antimicrob. Chemother. **4:**571–576.
40. **Anes E, Peyron P, Staali L, Jordao L, Gutierrez MG, Kress H, Hagedorn M, Maridonneau-Parini I, Skinner MA, Wildeman AG, Kalamidas SA, Kuehnel M, Griffiths G.** 2006. Dynamic life and death interactions between *Mycobacterium smegmatis* and J774 macrophages. Cell. Microbiol. **8:**939–960.
41. **Jordao L, Bleck CK, Mayorga L, Griffiths G, Anes E.** 2008. On the killing of mycobacteria by macrophages. Cell Microbiol. **10:**529–548.
42. **Torrelles JB, Sieling PA, Arcos J, Knaup R, Bartling C, Rajaram MV, Stenger S, Modlin RL, Schlesinger LS.** 2011. Structural differences in lipomannans from pathogenic and nonpathogenic mycobacteria that impact CD1b-restricted T cell response. J. Biol. Chem. **286:**35438–35446.
43. **de Lima R, Seabra AB, Durán N.** 2012. Silver nanoparticles: a brief review of cytotoxicity and genotoxicity of chemically and biogenically synthesized nanoparticles. J. Appl. Toxicol. **32:**867–879.
44. **Valodkar M, Bhadoria A, Pohnerkar J, Mohan M, Thakore S.** 2010. Morphology and antibacterial activity of carbohydrate-stabilized silver nanoparticles. Carbohydr. Res. **345:**1767–1773.
45. **Lemarchand C, Gref R, Passirani C, Garcion E, Petri B, Müller R, Costantini D, Couvreur P.** 2006. Influence of polysaccharide coating on the interactions of nanoparticles with biological systems. Biomaterials **27:**108–118.
46. **Kim TH, Kim M, Park HS, Shin US, Gong MS, Kim HW.** 2012. Size-dependent cellular toxicity of silver nanoparticles. J. Biomed. Mater. Res. A **100:**1033–1043.
47. **Carlson C, Hussain SM, Schrand AM, Braydich-Stolle LK, Hess KL, Jones RL, Schlager JJ.** 2008. Unique cellular interaction of silver nanoparticles: size-dependent generation of reactive oxygen species. J. Phys. Chem. B **112:**13608–13619.
48. **Bar-llan O, Albrecht RM, Fako VE, Furgeson DY.** 2009. Toxicity assessment of multisized gold and silver nanoparticles in zebra fish embryos. Small. **5:**1897–1910.
49. **Liu J, Sonshine DA, Shervani S, Hurt RH.** 2010. Controlled release of biologically active silver from nano silver surface. ACS Nano. **4:**6903–6913.
50. **Foldbjerg R, Dang DA, Autrup H.** 2011. Cytotoxicity and genotoxicity of silver nanoparticles in the human lung cancer cell line, A549. Arch. Toxicol. **85:**743–750.
51. **Kadiu I, Nowacek A, McMillan J, Gendelman HE.** 2011. Macrophage endocytic trafficking of antiretroviral nanoparticles. Nanomedicine (Lond.) **6:**975–994.
52. **Wang H, Wu L, Reinhard BM.** 2012. Scavenger receptor mediated endocytosis of silver nanoparticles into J774A.1 macrophages is heterogeneous. ACS Nano. **6:**7122–7132.
53. **Gratton SE, Ropp PA, Pohlhaus PD, Luft JC, Madden VJ, Napier ME, DeSimone JM.** 2008. The effect of particle design on cellular internalization pathways. Proc. Natl. Acad. Sci. U. S. A. **105:**11613–11618.
54. **Qui Y, Liu Y, Wang L, Xu L, Bai R, Ji Y, Wu X, Zhao Y, Li Y, Chen C.** 2010. Surface chemistry and aspect ratio mediated cellular uptake of Au nanorods. Biomaterials **31:**7606–7619.
55. **Chithrani BD, Ghazani AA, Chan WC.** 2006. Determining the size and shape dependence of gold nanoparticle uptake into mammalian cells. Nano. Lett. **6:**662–668.
56. **See V, Free P, Cesbron Y, Nativo P, Shaheen U, Rigden DJ, Spiller DG, Fernig DG, White MR, Prior IA, Brust M, Lounis B, Lévy R.** 2009. Cathepsin L digestion of nanobioconjugates upon endocytosis. ACS Nano. **3:**2461–2468.